Robust feedforward control of robotic arms with friction model uncertainty

Michiel Plooij *, Wouter Wolfslag and Martijn Wisse

** Corresponding author*
Delft University of Technology
Mekelweg 2
2628 CD Delft
The Netherlands
m.c.plooij@tudelft.nl, w.j.wolfslag@tudelft.nl, m.wisse@tudelft.nl

Abstract

To design feedforward controllers for robots, a model that includes friction is important. However, friction is hard to identify, which causes uncertainty in the model. In this paper we consider rest-to-rest motions of robotic arms that use only feedforward control. We show that it is possible to design feedforward controllers such that the final position of the motion is robust to uncertainty in the friction model. We studied a one DOF robotic arm in the horizontal plane, of which we show analytical, simulation and hardware results and we also show simulation results of a planar two DOF arm. Our friction model includes three types of friction: viscous, Coulomb and torque dependent friction. The results show that it is possible to eliminate the sensitivity of the final state to uncertainty in the three types of friction.

Keywords: Feedforward control, open loop control, robotic arms, model uncertainty, friction

1. Introduction

We are fascinated by the question what is still possible without feedback on robotic arms. Control without feedback is called feedforward control or open loop control. Although intuition tells us that accuracy in the presence of model uncertainty and disturbances using only feedforward control is hopeless, humans

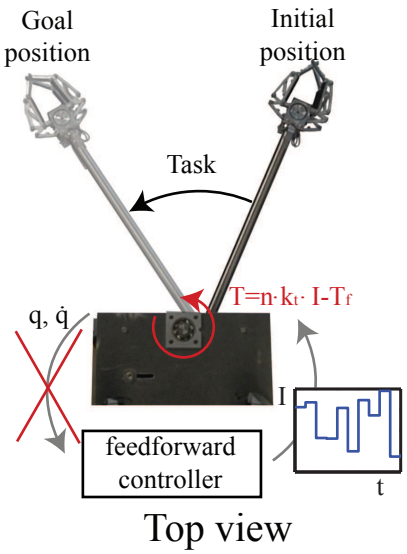

Figure 1: A schematic representation of the subject of this paper. The one DOF robotic arm in this picture has to perform a rest-to-rest motion: move from the initial to the goal position. The controller is a feedforward controller, which means that the state (i.e. position q and velocity $\dot{q}$) is not used to determine the control signal. The control signal is a current I, which is only a function of time. The resultant torque on the arm is the motor torque minus the friction torque. In this paper, we investigate the sensitivity of feedforward motions to uncertainty in the friction parameters. These model uncertainties usually cause the arm to end up in a different state than the goal state. We aim to eliminate this error in the final state. (figure from [1])

use feedforward control for fast motions and are still able to perform their tasks accurately [2]. In this paper, we present the surprising result that the final state of rest-to-rest motions of robotic arms can be made insensitive to uncertainty in the friction model. Possible fields of application include environments with heavy radiation, such as nuclear disaster areas or space, where feedback might be difficult and applications in which a large amount of agents are controlled with one input signal [3].

Generally, feedforward control laws use models of the system to compute control signals. These models often include friction, which is hard to model

accurately despite the amount of literature on friction identification [4, 5, 6, 7, 8]. Such inaccurate modeling introduces model uncertainty. Usually, the controller relies on feedback to compensate for uncertainty in the model. We are interested if it is also possible to incorporate robustness of the final position of motions to model uncertainty in the feedforward controller of robotic arms. As case studies, we use robotic arms with one and two DOF in the horizontal plane that are controlled with only a feedforward controller.

Multiple researchers share our fascination for only feedforward control and have shown positive results. Firstly, Schaal and Atkeson showed that it is possible to perform robot juggling with an open loop controller [9]. Seyfarth et al. showed a similar example in which feedforward control schemes for the swing leg retraction improved the stability of running in a humanoid robot [10]. And finally, Mombaur et al. showed that even stable walking and running are possible by creating open loop stable periodic motions [11, 12]. Although interesting, these researches did not account for model uncertainty.

Also robustness of feedforward controllers to model uncertainty has been studied before. Firstly, Singhose, Seering and Singer showed that input shaping to reduce vibrations can be performed in open loop while being robust to uncertainty in the natural frequency and damping of the system [13, 14]. Secondly, Akella and Mason showed that the result of several pushing actions in planar manipulation can be made robust to uncertainty in the initial position of the object [15]. Thirdly, Becker and Bretl showed that using open loop control on differential drive robots, the final position of a motion can be made robust to uncertainty in the wheel diameter [16]. They also showed that this works for balls with an uncertain diameter that roll over a moving plate [17]. All previous examples of feedforward control with robustness to model uncertainty concern systems with first order dynamics. Recently we showed the potential of using feedforward control on robotic arms with an inaccurate model, which is a second order system [1]. There is one technique all these examples use: a certain

task redundancy[1] is exploited in order to make the controller robust. We are continuing on the last example, by exploiting task redundancy in rest-to-rest motions of robotic arms.

Exploiting the task redundancy to compensate for model uncertainty has also been observed in humans. The human nervous system introduces large time delays of typically 150 ms [18, 19] and therefore humans must partially rely on feedforward control [2]. Since the internal model of humans is inaccurate [20] they exploit task redundancy to minimize the error due to model uncertainties. Error-minimizing feedforward signals have been reported in eye movements [21], but also in the games of darts and skittles [22, 23, 24, 25].

The task we consider in this paper is a pick-and-place task, which also possesses redundancy (see Fig. 1). The task consists of rest-to-rest motions where only the initial and final position matter and the path in between can be chosen freely. We demonstrate that by choosing the right feedforward controller, it is possible to essentially eliminate the sensitivity of the final state to uncertainty in the friction model.

We extend our research in [1] in three ways. Firstly, we start with an analytical approach to gain more understanding of the principles behind feedforward control of robotic arms with friction model uncertainty. Secondly, we show improved results on a one DOF simulation model with multiple uncertainties at the same time. And thirdly, we show simulation results on a two DOF simulation model. For completeness, we also show the hardware results from [1].

The rest of this paper is structured as follows. Section 2 provides the problem formulation of the problem that is considered in this paper. Sections 3, 4 and 5 show analytical, numerical and hardware studies respectively, on one and two DOF systems. The paper ends with a discussion in section 6 and a conclusion in section 7.

[1] Task redundancy means that there are multiple ways to fulfill the task perfectly.

2. Problem formulation

This section describes the problem of feedforward control with friction model uncertainty. First, the problem is formulated in general terms, then two case studies are introduced that will be studied in this paper and finally, the task description of the arms will be discussed.

2.1. General problem

We consider mechanical systems of the form

$$\dot{x}(t) = f(x(t), u(t), p) \tag{1}$$

where x is the state containing the positions q and the velocities $\dot{q}$, u is the input and p are the friction parameters. The motions we consider have an initial state x_0 and a final state x_f, leading to the following initial condition and motion constraint:

$$x(0) = x_0 = \begin{bmatrix} q_0 \\ \dot{q}_0 \end{bmatrix} \tag{2}$$

$$x(t_f) = x_f = \begin{bmatrix} q_f \\ \dot{q}_f \end{bmatrix} \tag{3}$$

where t_f is the time to move. We now define y as the state at t_f, which is a function of x_0, u and p:

$$y(x_0, u(t), p) = x(t_f) = x(0) + \int_0^{t_f} f(x(\tau), u(\tau), p) d\tau \tag{4}$$

The goal is to make the final state of the arm insensitive to the friction parameters. We define sensitivity as:

$$S_{ij} = \left| \frac{\partial y_j(x_0, u(t), p)}{\partial p_i} \right| \tag{5}$$

$$S(u(t)) = \sum_{i=1}^{i=k} \sum_{j=1}^{j=n} c_{ij} S_{ij} \tag{6}$$

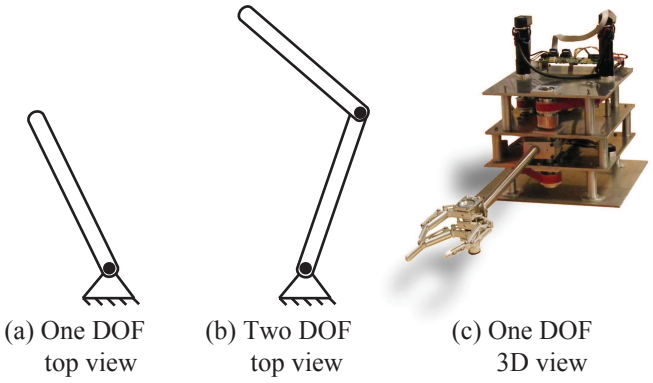

Figure 2: The three configurations we studied: (a) Simulation models of a one DOF arm in the horizontal plane. (b) A simulation model of a two DOF system in the horizontal plane. (c) Hardware experiments on a one DOF robotic arm to show that the principles found in the simulation studies work on a hardware setup.

where S_{ij} is the sensitivity of final state j to parameter i, S is the total sensitivity and c_{ij} is the weighing factor corresponding to parameter p_i and the jth state. In this paper we weigh all sensitivities equally, meaning that c_{ij}=1 for all i and j. The sensitivity S_{ij} is equal to zero when the final state j is insensitive to the friction parameter p_i. Note that this definition differs from the classical definition of sensitivity in control [26]. This goal can be transformed into an optimization as follows:

$$\begin{aligned} \underset{u(t)}{\text{minimize}} \quad & S(u(t)) \\ \text{subject to} \quad & |u(t)| \leq u_{max} \qquad \forall t \\ & q(t_f) = q_f \\ & \dot{q}(t_f) = \dot{q}_f \end{aligned} \tag{7}$$

where k is the number of friction parameters, n is the number of states, and u_{max} is the maximum input.

2.2. Case studies

There are two case studies we consider in this paper: a one DOF arm and a two DOF arm, both in the horizontal plane (see Fig. 2a and 2b). We also show results from hardware experiments on a one DOF arm to confirm the results from simulation (see Fig. 2c).

The equations of motion of the models will be given in the sections discussing the specific models (sections 3.1, 3.2, 4.1 and 4.2). In all models, the actuation torque applied by the DC motors on the joints is equal to:

$$T = nk_tI \tag{8}$$

Where T is the actuation torque k_t is the motor constant, n is the gearbox ratio and I is the current through the motor. Since we use motor controllers with current control, the current is used as the input u.

Our frictional model consists of three commonly used types of friction: viscous friction, Coulomb friction and torque dependent friction:

$$T_p = \left\{ \begin{array}{ll} p_v\dot{q} + \text{sign}(\dot{q})(p_c + p_t|T|) & \text{for } \dot{q} \neq 0 \\ \min(p_c + p_t|T|; |T|)\text{sign}(T) & \text{for } \dot{q} = 0 \end{array} \right\} \tag{9}$$

where T_p is the frictional torque, p_v is the viscous friction coefficient, p_c is the Coulomb friction constant and p_t is the torque dependent friction coefficient. Torque dependent friction is less commonly used than the other two. The way we use it is similar to the force dependent friction term in [5]. We included this type of friction because model identification showed the presence of torque dependent friction.

2.3. Task description

We consider rest-to-rest motions, which are very common motions for robotic arms. For instance, in industry pick-and-place tasks depend on accurate rest-to-rest motions. In practice, a robotic arm performing rest-to-rest motions has to move between a number of positions. In the analytical studies, we will keep the

task description generic. In the numerical results, we will show specific results where the one DOF arm moves from 0 rad to 1 rad and the two DOF arm moves from $[-0.5, 0]$ rad to $[0.5, 0]$ rad, all with a time to move of $t_f = 1$s. In the one DOF case, we will analyse how the results change when changing the task. This will show that other initial and goal positions lead to identical results as long as the distance between the two does not exceed a certain threshold.

3. Analytical Studies

In this section, we study the problem analytically, in order to understand the principles behind feedforward control of robotic arms with friction model uncertainty. For this purpose, we study two one-DOF models: a model with only viscous friction and a model with only Coulomb friction. The first model is a negative example, showing that for this model uncertainty in the viscous friction cannot be compensated for. The second model is a positive example, showing that uncertainty in the Coulomb friction can be compensated for.

3.1. With only viscous friction

In the one DOF model with only viscous friction, the equations of motion are:

$$\frac{d}{dt}\begin{bmatrix} q \\ \dot{q} \end{bmatrix} = \begin{bmatrix} \dot{q} \\ \frac{1}{J_{joint}}(k_t n I - p_v \dot{q}) \end{bmatrix} \tag{10}$$

where J_{joint} is the inertia about the joint. If we now integrate the second row of this equation with respect to time we get

$$J_{joint}\ddot{q} = k_t n I(t) - p_v \dot{q} \tag{11}$$

$$J_{joint}\Delta\dot{q} = \int k_t n I(t) dt - p_v \Delta q = 0 \tag{12}$$

where Δq is the change in angular position and $\Delta\dot{q}$ is the change in angular velocity. $\Delta\dot{q}$ is equal to zero since we start and end with zero velocity. Here, $I(t)$

can be chosen freely, as long as the motion satisfies the constraints in (7). Suppose that $I^*(t)$ is a feedforward control signal that satisfies the constraints and add $\delta(t)$ to the signal, which represents all possible changes in the feedforward control signal:

$$\Delta q = \frac{k_t n}{p_v} \int (I^*(t) + \delta(t)) dt \tag{13}$$

$$= \frac{k_t n}{p_v} \left(\int I^*(t) dt + \int \delta(t) dt \right) \tag{14}$$

Since the final position of the motion should not change in order to satisfy (7), all possible changes $\delta(t)$ of the feedforward control signal are constrained by the following equation:

$$\int \delta(t) dt = 0 \tag{15}$$

Combining (14) and (15), leads to

$$\Delta q = \frac{k_t n}{p_v} \int I^*(t) dt \tag{16}$$

From (16), we see that $\dfrac{\partial \Delta q}{\partial p_v}$ is independent of changes of the feedforward control signal that reach the same end state for the nominal value of p_v. This shows that all the changes in the feedforward control signal that satisfy the constraints, do not influence the sensitivity of the final position of the arm to the viscous friction.

Apparently, on the system we are considering it is impossible to achieve the goal of this paper: sensitivity of the feedforward motion to uncertainty in the friction model is independent of the chosen feedforward controller.

3.2. With only Coulomb friction

So now consider a one DOF system with only Coulomb friction. In this system, the equations of motion are:

$$\frac{d}{dt}\begin{bmatrix} q \\ \dot{q} \end{bmatrix} = \begin{bmatrix} \dot{q} \\ \frac{1}{J_{joint}}(I(t)k_t - p_c \text{sign}(\dot{q})) \end{bmatrix} \tag{17}$$

The changes in velocity and position are equal to:

$$\Delta\dot{q} = \int \frac{I(t)k_t n}{J_{joint}}\,\mathrm{d}t - p_c \int \frac{\text{sign}(\dot{q})}{J_{joint}}\,\mathrm{d}t \tag{18}$$

$$\Delta q \quad = \quad \iint \frac{I(t)k_t n}{J_{joint}}\,\mathrm{d}t^2 - p_c \iint \frac{\text{sign}(\dot{q})}{J_{joint}}\,\mathrm{d}t^2 \tag{19}$$

In (18) and (19), we see that there are three components that influence the final position of the arm: the current through the motor, the sign of the velocity and the amplitude of the Coulomb friction p_c. Note that the Coulomb friction is a bang-bang torque. A change in the Coulomb friction constant has two effects:

1. The amplitude of the bang-bang Coulomb friction torque scales
2. The switch times of the sign($\dot{q}$) function change.

If we assume the second effect is negligible, then the total effect of changing the Coulomb friction is a scaling of the frictional term in (18) and (19). If we now choose our feedforward control signal such that:

$$\int \text{sign}(\dot{q})\,\mathrm{d}t = 0 \tag{20}$$

and

$$\iint \text{sign}(\dot{q})\,\mathrm{d}t^2 = 0 \tag{21}$$

then a change in the amplitude of the Coulomb friction torque has no effect on the final position and velocity.

The assumption above is not valid, as we will now show with an example, but does lead to small values of the partial derivatives in (5). To show this, we used a simulation of a robotic arm of which the parameters are given in Table 1. Fig. 3

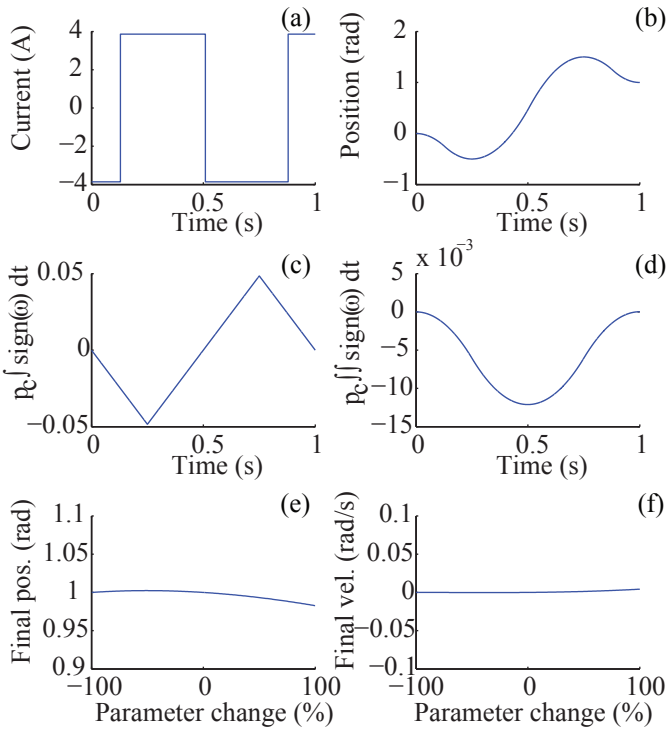

Figure 3: A simple example of a motion that satisfies the requirements to eliminate the effect of an uncertain Coulomb friction on the final position and velocity. Both the single and the double integral of the Coulomb friction over the time are approximately equal to zero. They are not exactly equal to zero, because the amplitude of the Coulomb friction also influences the zero crossing of the angular velocity. (a) The current through the motor as function of time. (b) The position of the arm as function of time using the nominal friction values. (c) The integral of the Coulomb friction over time. (d) The double integral of the Coulomb friction over time. (e) the final position of the arm as function of the Coulomb friction parameter change. (f) the final velocity of the arm as function of the Coulomb friction parameter change.

shows a motion that satisfies Eqs. (20) and (21). The motion has three phases: first, it starts with a negative velocity, second, it continues with a positive velocity and finally, it ends with a negative velocity again. Figs. 3e and 3f show that the derivatives of the final position and velocity to the Coulomb friction are approximately zero (0.009 $(\text{Nms})^{-1}$ and 0.012 $(\text{Nm})^{-1}$). The derivatives are not exactly equal to zero because of the change in switch times.

Table 1: The model parameters of the arm with only Coulomb friction. All inertial terms are combined in the inertia about the joint (J_{joint}).

Parameter	Symbol	Value
Viscous friction	p_v	0 Nms/rad
Coulomb friction	p_c	0.19 Nm
Torque dependent friction	p_t	0 %
Inertia	J_{joint}	0.17 kgm^2
Motor constant	k_t	26.7 mNm/A
Gearbox ratio	n	1:54

4. Numerical Studies

In the previous section, we showed analytical results for a one DOF system with only viscous friction or with only Coulomb friction. However, when the complete friction model is considered (i.e. viscous, Coulomb and torque dependent friction) or when the dynamics are non-linear, obtaining analytical results becomes infeasible. Therefore, in this section, we perform numerical studies with a complete friction model (viscous, Coulomb and torque dependent friction). Although we showed in the previous section that in a system with only viscous friction, uncertainty in the viscous friction cannot be compensated for by the choice of the feedforward controller, in this section we will show that compensation is possible when the two other friction terms are non-zero. The two systems we consider are a one DOF robotic arm and a two DOF robotic arm. We will show that on both systems, the sensitivity to all three friction model uncertainties can be eliminated.

4.1. One DOF robotic arm

4.1.1. Method

The equations of motion for the one DOF model with complete friction model are given by

Table 2: The model parameters of the arm with the complete friction model, based on a system identification of our one DOF arm. All inertial terms are combined in the inertia about the joint (J_{joint}).

Parameter	Symbol	Value
Viscous friction	p_v	-0.05 Nms/rad
Coulomb friction	p_c	0.19 Nm
Torque dependent friction	p_t	22 %
Inertia	J_{joint}	0.17 kgm^2
Motor constant	k_t	26.7 mNm/A
Gearbox ratio	n	1:54
Maximum current	I_{max}	10 A

$$\frac{d}{dt}\begin{bmatrix} q \\ \dot{q} \end{bmatrix} = \begin{bmatrix} \dot{q} \\ \left(\frac{k_t n I - T_p}{J_{joint}}\right) \end{bmatrix} \tag{22}$$

where T_p is the frictional torque from Eq. (9). For the one DOF numerical study, we used the parameters values in Table 2, which are based on a system identification of the robotic arm in Fig. 2c.

The sensitivities in Eq. (5) are calculated using a finite difference approximation, with a 0.1% difference in the model parameters. In the numerical optimizations, we parameterized the controller as a piecewise constant current signal with N controller steps of equal length. An example of an input signal with $N = 3$ is shown in Fig. 4. These N controller steps are used as decision variables in the optimization in Eq. (7), constrained by Eq. (7). Since numerical optimization does not exactly reach zero, we set a threshold below which we call the outcome of an optimization equal to zero. This threshold is equal to the function tolerance of the optimization algorithm, which was set to 10^{-6}.

We used two techniques to speed up the optimizations. Firstly, instead of propagating the equations of motion using an ODE solver, we used the fact that the equations of motion of this one DOF system are piecewise linear, with switching times at changes in control signal and when the velocity crosses zero.

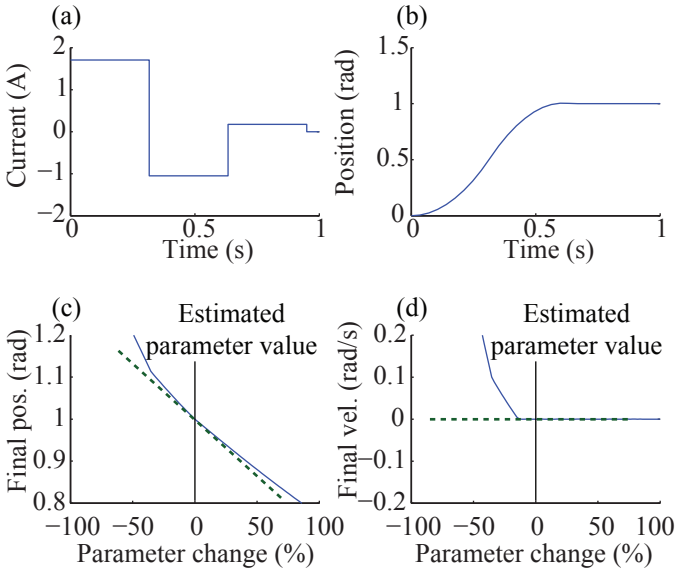

Figure 4: An example of a feedforward control signal and the motion that results from the controller. The signal represents the current through the motor as function of the time. There are 4 set points in total ($t_0 \dots t_3$) and the current is constant in between the set points. The duration of the signal is 1 second. (b) Shows the position of the arm as function of time using the nominal friction values. (c) and (d) show the final position and final velocity as function of the parameter value of the Coulomb friction. The green dotted lines show the partial derivatives of the final position and velocity with respect to the parameter value. The goal of the optimization is to minimize a weighed sum of these derivatives

Therefore we can calculate the exact end state with a number of calculation steps smaller than $2N$. Secondly, we made use of the fact that the goal velocity of rest-to-rest motions is zero ($\dot{q}_f = 0$). Due to the Coulomb friction in the system, an infinitely small velocity will be reduced to zero by coasting ($u = 0$) for a small amount of time. Therefore, in order to satisfy $\frac{\partial \dot{q}_f}{\partial p} = 0$, we let the system coast from $t = t_f - 0.05s$ to $t = t_f$. Now the optimization has to satisfy two equality constraints (see Eq. (7)) and has to minimize one partial derivative per uncertain parameter ($\frac{\partial q_f}{\partial p_i}$). Therefore, we used $N = 2 + k$ where k is the number of uncertain parameters.

The optimizations were performed with a multistart of the MATLAB function `fmincon` and were run on an Intel DuoCore i7-2620M CPU.

4.1.2. Results

Firstly, we obtained results with only one uncertain parameter at a time and thus $N = 3$. The 50 starts of the optimization had an average duration of 26 ms. In all the three optimizations, the partial derivatives (Eq. (5)) were all smaller than 10^{-9} which is smaller than the function tolerance of the optimization algorithm and are therefore considered zero. Lowering the function tolerance to 10^{-12} did lower the partial derivatives to 10^{-13}, while the motions did not change significantly. We chose to use the slightly larger function tolerance of 10^{-6} to keep the computational cost low. The results with an uncertain Coulomb friction are shown in Fig. 5. It shows that the final position of the arm is approximately 1 rad, even if p_c changes with 100% of the estimated value. Furthermore, it shows that the arm first moves away from the goal position, before moving towards it. We observed this behavior in all the three cases: with an uncertain p_v, p_c and p_t. Although optimization results can be hard to interpret, we saw the same behavior in the previous section in Fig. 3. Therefore, in all the three cases, probably some kind of condition as in Eq. (19) is satisfied.

Fig. 6 shows the partial derivatives as function of the goal position. It shows that every partial derivative is zero up until a certain threshold of the goal position. This threshold is smallest for the viscous friction (approximately 1.8 rad), is slightly larger for the torque dependent friction (approximately 2.3 rad) and is largest for the Coulomb friction (approximately 6 rad). These values depend on the amount of friction, the inertia and the maximum torque. The latter is a combination of the motor constant, the gearbox ratio and the maximum current.

Secondly, we obtained results with three uncertain parameters at the same time and thus $N = 5$. The 100 starts of the optimization had an average duration of 53 ms. The results of the optimization are shown in Fig. 7. We again see that the arm first moves away from the goal position. This was to be expected since the three separate optimizations showed this behavior. Furthermore, Fig. 7 shows that the final position is most sensitive to an uncertain torque dependent

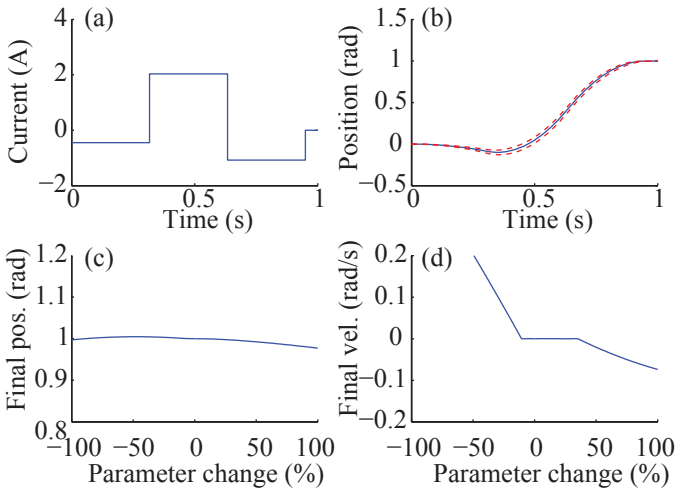

Figure 5: The results of the optimization with an uncertain Coulomb friction. (a) The current through the motor as function of time. (b) The position of the arm as function of time using the nominal friction values. The red striped lines show the position over time with -40% and +40% parameter change. (c) The final position as function of the parameter value of the Coulomb friction. (d) The final velocity as function of the parameter value of the Coulomb friction. The two bottom graphs show that the partial derivatives of the final state with respect to the parameter are zero.

friction. The partial derivatives (Eq. (5)) were all zero.

4.2. Two DOF robotic arm

4.2.1. Methods

We performed the same optimizations as on the one DOF model on a two DOF SCARA type arm model (see Fig. 8), to see how the results extrapolate to a robotic arm with non-linear dynamics. We used the TMT method [27] to obtain the equations of motion of the two DOF simulation model, which are too long to include in this paper. In the two DOF model, a motor actuates the absolute angle of the second joint. Since approximately all friction is caused by the motor, the friction in the second joint is a function of the absolute angular velocity of that joint. The friction between the first link and the second link is assumed to be zero.

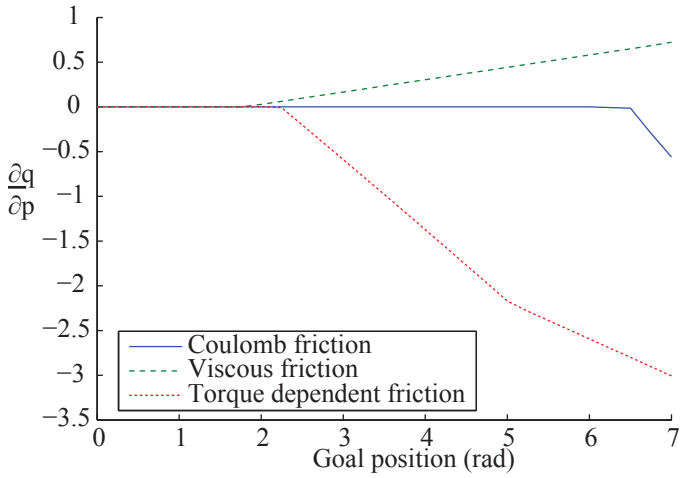

Figure 6: This figure shows the partial derivative of the goal position to the parameter changes as function of the goal position. The partial derivatives for all the three parameter variations are zero until a certain threshold on the goal position.

Table 3: The model parameters of the two DOF arm.

Parameter	Symbols	Values	Unit
Viscous friction	p_{v1}, p_{v2}	-0.05, -0.14	Nms/rad
Coulomb friction	p_{c1}, p_{c2}	0.19, 0.60	Nm
Torque dependent friction	p_{t1}, p_{t2}	22, 32	%
Inertia about COM	J_{C1}, J_{C2}	0.023, 0.178	kgm^2
Mass upper arm	m_1, m_2	0.809, 1.502	kg
Length of link upper arm	l_1, l_2	0.41, 0.43	m
Position COM	l_{C1}, l_{C2}	0.07, 0.33	m
Motor constant	k_{t1}, k_{t2}	26.7, 28.1	mNm/A
Gearbox ratio	n_1, n_2	1:54, 1:198	
Maximum current	I_{max1}, I_{max2}	10, 10	A

The parameter values of the two DOF model are listed in Table 3. In this model, there are multiple parameters that influence the inertia of the upper and lower arm: the inertias about the centers of mass (COMs), the lengths of the arms, the masses of the arms and the positions of the COMs. The 3

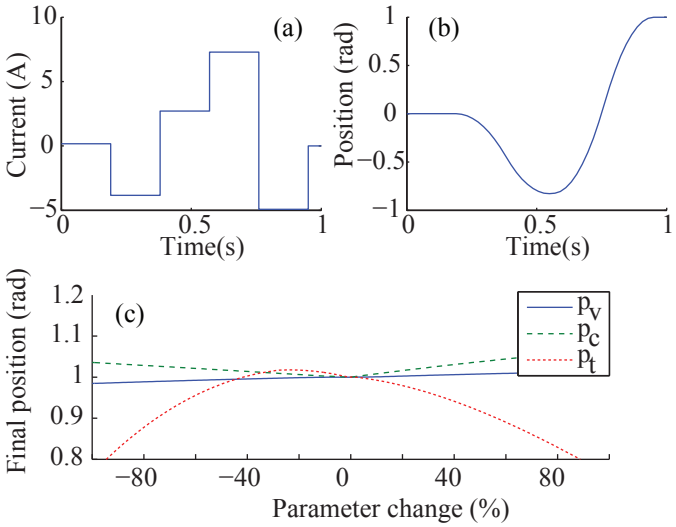

Figure 7: The results of the optimization on a one DOF arm with three uncertain friction parameters at the same time. (a) The current through the motor as function of time. (b) the position of the arm as function of time using the nominal friction values. (c) The final position of the arm as function of the three parameter changes. The bottom graph shows that the partial derivatives of the final position with respect to the three parameters values are zero.

friction parameters per joint lead to 6 uncertain parameters and thus 12 partial derivatives that should be equal to zero. Therefore, on both joints we took $N = 8$.

4.2.2. Results

Figs. 9c and 9d show the final positions of the two arms as functions of the parameter changes. The values of the partial derivatives are smaller than the function tolerance of the optimization and are therefore considered zero.

Figs. 9b shows the positions of the two joints as functions of time. The first joint shows the same behavior as the one DOF system: it first moves away from the goal position before moving towards it.

One optimization of the two DOF system takes about 10 hours, with the current state of technology, which is too long to be applicable. We will discuss this issue in section 6.

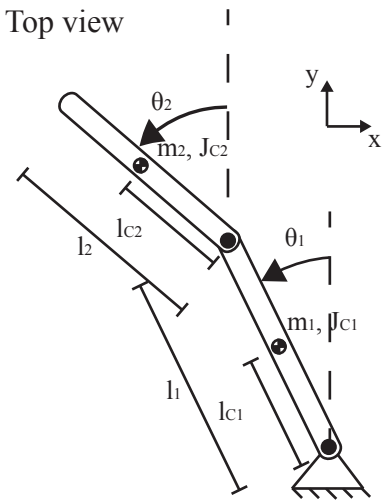

Figure 8: Top view of the two DOF SCARA type arm model. The second joint is actuated through a parallel mechanism (not shown in this figure), such that the angle of the second arm is an absolute angle. The friction acts on the absolute angles of the joints.

5. Hardware Study

In the previous sections we saw that in theory, feedforward controlled motions of our robotic arm can be made insensitive to friction model uncertainty. In this section, we show that this is also possible on the robotic arm itself. We verify the results with an uncertain Coulomb friction on our one DOF robotic arm and show that the sensitivity to this friction uncertainty can be eliminated to negligible levels. Firstly, we will explain the test set up, secondly, we will explain our test protocol and finally, we will show the results.

5.1. The robotic arm

Fig. 2c shows a picture of the one DOF robotic arm, which is the same arm as in [28], but without the spring mechanism. The DOF consists of an 18x1.5mm stainless steel tube connected with a joint to the ground. A weight of 1 kg is connected to the end of the tube, which represents the weight of a gripper plus a product. The motor is placed on a housing and AT3-gen III 16mm timing belts are used to transfer torques within the housing. The joint is actuated by a

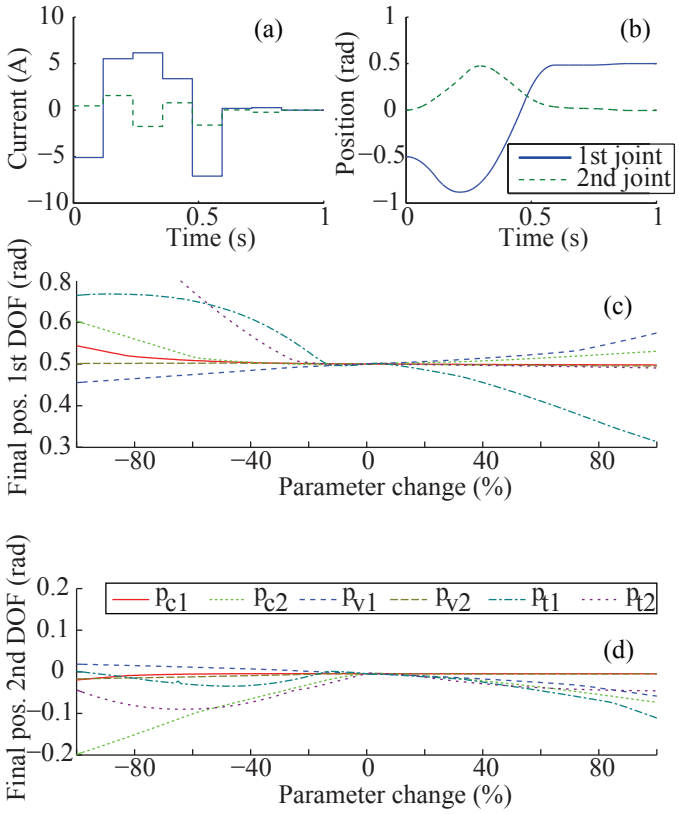

Figure 9: The results of the optimization on a two DOF arm with three uncertain friction parameters at the same time. (a) The currents through the motors as function of time. (b) the positions of the joints as function of time using the nominal friction values. (c) The final position of the first joint as function of the six parameter changes. (d) The final position of the second joint as function of the six parameter changes. The two bottom graphs show that the partial derivatives of the final position with respect to the parameters values are approximately zero.

Maxon 60W RE30 motor with a gearbox ratio of 18:1. The timing belts provide an additional transfer ratio of 3:1. The model parameters as shown in Table 2 are based on a system identification of this robotic arm.

To change the Coulomb friction, we designed a mechanism that adds Coulomb friction by clamping a nylon sleeve bearing on the motor axis. The Coulomb friction can be increased by tightening the screw of the clamping mechanism.

Every time after we changed the Coulomb friction, we ran a system identification to determine the amount of friction that was added.

5.2. Test protocol

We performed an online optimization to find the feedforward controller that is most robust to uncertainty in the Coulomb friction. This optimization consisted of testing a grid of 32 different feedforward controllers and selecting the best one. Each feedforward controller had three current set points of which the first one was determined by a grid of 32 set points. The other two set points were determined by the constraints on the final position and final velocity in simulation.

Instead of using the derivative as a performance measure, we used the root mean squared (RMS) of the position errors using three different values for the Coulomb friction: 0.19 Nm, 0.22 Nm and 0.25 Nm.

5.3. Results

Fig. 10 shows the current and the position as function of time for a typical experimental run. The two controllers shown are the two resulting in the minimum and maximum errors in the hardware experiments. It also shows that the current profiles with minimal and maximal error in hardware experiments correspond to the current profiles with minimized and maximized sensitivity in simulation. For systems with more DOFs it is less feasible to perform a grid search and thus the current profiles from simulation should be used.

The minimal and maximal RMS were 0.002 rad and 0.092 rad respectively. These hardware experiments confirm the main conclusions of the simulation study: the errors due to uncertainty in the friction model can be reduced to approximately zero (at least for the Coulomb friction). Furthermore, again the optimal motion first moves in negative direction before moving towards the goal position.

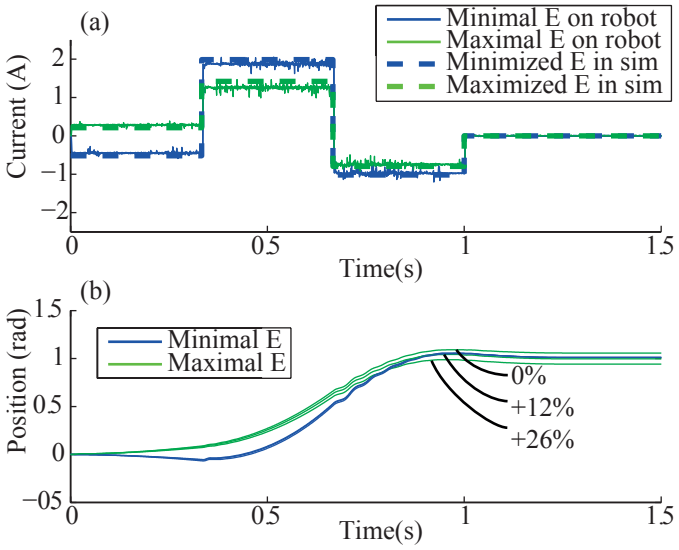

Figure 10: A typical example of the data obtained from hardware experiments. This figure shows the minimized and maximized motions for a changing Coulomb friction. a) The feedforward current as function of the time. The solid lines correspond to the motions with minimized and maximized error in hardware experiments. The dashed lines are optimized current profiles in simulation. This graph shows that the current profiles optimized in simulation are the same as the current profiles with minimal and maximal error in hardware experiments. b) The position of the arm as function of the time. We clearly see that the spread in the final position of the minimized motion is smaller than that of the maximized motion. For the minimized motion, it is hard to distinguish the three lines, for the maximized motion the spread is clearly visible. (Figure from [1])

6. Discussion

In this study we researched motions of a one and two DOF robotic arm, controlled by a feedforward controller. The task consisted of fixed initial and goal positions and a fixed time per stroke. We showed that the choice of the motions in between the initial and goal positions is important for the sensitivity of the final state to friction model uncertainty. For all systems, this sensitivity can be eliminated.

6.1. Implications

The results of this study are important to consider when implementing feedforward control. The correct use of feedforward control improves the performance of the system and this study shows that the performance can even be improved in such a way that the friction parameters do not have to be known accurately. The interesting result is that all optimized motions do not move from the initial to the goal position directly, but first move away from the goal position. We showed why this strategy is advantageous in one DOF with an uncertain Coulomb friction and we expect that similar explanations hold for other friction uncertainties and systems.

This study also has implications on the field of human motion control. Recent studies in the field of human motion control focused on the uncertainty (i.e. noise) in the control signals [21]. It would be interesting to research the accuracy of the internal models of humans and the influence of this accuracy on the motions humans choose. Another interesting topic for future research would be the influence of noise on the performance of feedforward control in robotic systems.

The one DOF system is a system with linear dynamics and non-linear friction and the two DOF system is a system with non-linear dynamics. We expect that the results of this research can be extrapolated to a variety of other systems. We did not consider gravity in this study. Adding DOFs that are influenced by the gravity adds non-linearity to the system. We expect that sensitivity minimizing feedforward controllers can still be found on such systems.

6.2. Linearization

In this study, we used a linearization of the influence of a parameter on the final state as a measure of the performance of a feedforward controller. This linearization only accounts for infinitely small parameter changes and thus it does not tell anything about finite parameter changes. However, many of our results showed that the errors in the final position were even small with large parameter changes (see e.g. Fig 5 and Fig. 7). A first alternative to linearizing

is to sample a couple of parameter values around the estimated value (e.g. estimated value -10% and estimated value +10%) and minimize a sum or RMS of the errors at those parameter values, as we did in [1]. However, such an optimization takes longer since more decision variables are needed. A second alternative would be to also take into account higher order partial derivatives, as in [16]. We do not expect that this will lead to a better performance since the results already show a low second order derivative (see Figs. 5, 7 and 9).

6.3. Adding feedback

In most applications, some kind of feedback is available. Combining a separately designed feedback controller and a robust feedfoward controller will in general not lead to good results, since in general the superposition principle does not hold. An approach could be to first design a feedback controller and then optimize the combination of that controller with a feedforward controller to be robust to model uncertainty. Although showing the feasibility of this approach is part of future work, an interesting approach was recently proposed by Ansari and Murphey [29].

6.4. Optimization duration

For the one DOF system, the duration of one optimization was 5.3 seconds. This is still too slow for performing optimizations while the arm is performing its task. However, there are obvious ways to solve this problem, like creating a database of motions and only use the optimization to adjust the closest motion from the database to fit the required motion. Such an optimization should not require a multistart and should therefore take about 50 ms for the considered system. In general, the optimization would be fast enough if the optimization time is shorter than the time to move, which in our example was 1s.

A problem arises when the systems become more complex: more DOFs or more uncertain parameters. An example of this is the two DOF system in section 4.2, for which an optimization had to run for 10 hours to find a reasonable solution. This problem is caused by the large number of local minima in the

optimization function. These local minima are caused by a combination of highly non-linear dynamics and a relatively large number of decision variables. Although this problem is suited for parallelization, it would require more than 36000 cores to speed up the optimization to 1 second per motion. Therefore, the best approach would be to search for methods that do not have this large amount of local minima.

Because of this large optimization time, we did not perform an elaborate two DOF study on the influence that the initial and goal positions have on the results. However, trying a couple of random tasks showed that similar results can be obtained for other tasks. We expect that what we showed for the one DOF system, also holds for the two DOF system: the sensitivity can be reduced to zero if the distance between initial and goal positions does not exceed a certain threshold.

6.5. Other optimization goals

In this paper, we optimized feedforward controllers such that the sensitivity to friction model uncertainty was minimized. However, both in industry and in human motion control, other cost functions are used as well. Two common cost functions are the time per stroke and the energy consumption per stroke. The question that remains is how these commonly used cost functions perform with an uncertain friction model in comparison to the results of the optimization in this paper.

Fig. 11 shows the energy and time optimal motions of the one DOF system with a complete friction model. The time optimal torque profile was obtained by minimizing the time the system reaches the goal state. The energy optimal torque profile was obtained by minimizing the integral of the electrical motor power over time (see [28]). The values of the partial derivatives are shown in Table 4. This shows that both the energy and time optimal motions are very sensitive to friction model inaccuracies, and so a trade-off has to be made between energy, time and robustness.

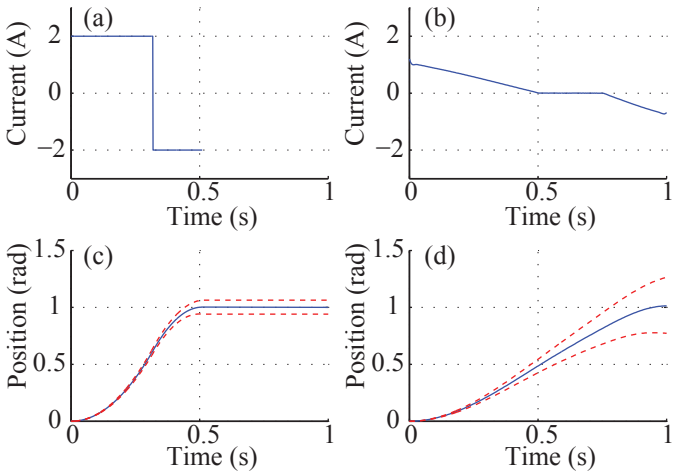

Figure 11: The time and energy optimal motions as function of time. (a) The current through the motor of the time optimal motion. (b) The current through the motor of the energy optimal motion. (c) The position of the arm of the time optimal motion. (d) The position of the arm of the energy optimal motion. The red striped lines show the position over time with -40% and +40% parameter change.

Table 4: The partial derivatives of energy and time optimal motions

	p_c	p_v	p_t
Energy optimal			
$\frac{\partial q}{\partial p_i}$	-0.626	0.163	-0.499
$\frac{\partial \dot{q}}{\partial p_i}$	-1.318	0.357	-0.839
Time optimal			
$\frac{\partial q}{\partial p_i}$	-0.154	0.074	-0.499
$\frac{\partial \dot{q}}{\partial p_i}$	-0.344	0.180	-1.109

7. Conclusion

In this paper, we optimized feedforward controllers for robustness to uncertainty in the friction model. On both the one and two DOF system, we eliminated the sensitivity of the final position of rest-to-rest motions to parametric uncertainty in the friction model. Interestingly, all motions that are

robust to friction model uncertainty, first move away from the goal position before moving towards it. Such motions eliminate the sensitivity by reducing the integral of the effect of the friction torque to zero.

Acknowledgement

This work is part of the research programme STW, which is (partly) financed by the Netherlands Organisation for Scientific Research (NWO).

[1] M. Plooij, M. De Vries, W. Wolfslag, M. Wisse, Optimization of feedforward controllers to minimize sensitivity to model inaccuracies, in: Intelligent Robots and Systems (IROS), Proceedings of the IEEE/RSJ International Conference on, 2013.

[2] M. Desmurget, S. Grafton, Forward modeling allows feedback control for fast reaching movements, Trends in cognitive sciences 4 (11) (2000) 423–431.

[3] A. Becker, O. Felfoul, P. Dupont, Simultaneously powering and controlling many actuators with a clinical mri scanner, in: Intelligent Robots and Systems (IROS), IEEE/RSJ International Conference on, 2014, pp. 2017–2023.

[4] P. Dahl, A solid friction model, Tech. rep., DTIC Document (1968).

[5] P. E. Dupont, The effect of coulomb friction on the existence and uniqueness of the forward dynamics problem, in: Robotics and Automation, Proceedings of the IEEE International Conference on, IEEE, 1992, pp. 1442–1447.

[6] P. Bliman, M. Sorine, Friction modeling by hysteresis operators. application to dahl, sticktion and stribeck effects, Pitman Research Notes in Mathematics Series (1993) 10–10.

[7] H. Olsson, K. J. Åström, C. Canudas de Wit, M. Gäfvert, P. Lischinsky, Friction models and friction compensation, European journal of control 4 (3) (1998) 176–195.

[8] E. Berger, Friction modeling for dynamic system simulation, Applied Mechanics Reviews 55 (6) (2002) 535–577.

[9] S. Schaal, C. Atkeson, Open loop stable control strategies for robot juggling, in: Robotics and Automation, Proceedings of the IEEE International Conference on, 1993, pp. 913 –918 vol.3.

[10] A. Seyfarth, H. Geyer, H. Herr, Swing-leg retraction: a simple control model for stable running, Journal of Experimental Biology 206 (15) (2003) 2547–2555.

[11] K. Mombaur, R. Longman, H. Bock, J. Schlöder, Open-loop stable running, Robotica 23 (1) (2005) 21–33.

[12] K. D. Mombaur, H. G. Bock, J. P. Schlöder, R. W. Longman, Open-loop stable solutions of periodic optimal control problems in robotics, ZAMM-Journal of Applied Mathematics and Mechanics/Zeitschrift für Angewandte Mathematik und Mechanik 85 (7) (2005) 499–515.

[13] N. C. Singer, W. P. Seering, Preshaping command inputs to reduce system vibration, Journal of Dynamic Systems, Measurement, and Control 112 (1990) 76–82.

[14] W. Singhose, W. Seering, N. Singer, Residual vibration reduction using vector diagrams to generate shaped inputs, Journal of Mechanical Design 116 (1994) 654–659.

[15] S. Akella, M. T. Mason, Posing polygonal objects in the plane by pushing, in: Robotics and Automation, Proceedings of the IEEE International Conference on, IEEE, 1992, pp. 2255–2262.

[16] A. Becker, T. Bretl, Approximate steering of a unicycle under bounded model perturbation using ensemble control, IEEE Transactions on Robotics 28 (3) (2012) 580–591.

[17] A. Becker, T. Bretl, Approximate steering of a plate-ball system under bounded model perturbation using ensemble control, in: Intelligent Robots and Systems (IROS), IEEE/RSJ International Conference on, 2012, pp. 5353–5359.

[18] S. Thorpe, D. Fize, C. Marlot, Speed of processing in the human visual system, Nature 381 (6582) (1996) 520–522.

[19] P. Cordo, L. Carlton, L. Bevan, M. Carlton, G. K. Kerr, Proprioceptive coordination of movement sequences: role of velocity and position information, Journal of Neurophysiology 71 (5) (1994) 1848–1861.

[20] M. Kawato, Internal models for motor control and trajectory planning, Current Opinion in Neurobiology 9 (6) (1999) 718 – 727.

[21] C. M. Harris, D. M. Wolpert, Signal-dependent noise determines motor planning, Nature 394 (6695) (1998) 780–784.

[22] J. Smeets, M. Frens, E. Brenner, Throwing darts: timing is not the limiting factor, Experimental Brain Research 144 (2002) 268–274.

[23] H. Müller, E. Loosch, Functional variability and an equifinal path of movement during targeted throwing, Journal of Human Movement Studies 36 (1999) 103–126.

[24] H. Müller, D. Sternad, Decomposition of variability in the execution of goal-oriented tasks: Three components of skill improvement., Journal of Experimental Psychology: Human Perception and Performance 30 (1) (2004) 212–233.

[25] R. G. Cohen, D. Sternad, State space analysis of timing: exploiting task redundancy to reduce sensitivity to timing, Journal of Neurophysiology 107 (2) (2012) 618–627.

[26] B. Friedland, Control system design: an introduction to state-space methods, Courier Corporation, 2012.

[27] R. van der Linde, A. Schwab, Lecture notes on multibody dynamics b, wb1413, Delft University of Technology.

[28] M. Plooij, M. Wisse, A novel spring mechanism to reduce energy consumption of robotic arms, in: Intelligent Robots and Systems (IROS), Proceedings of the IEEE/RSJ International Conference on, 2012, pp. 2901–2908.

[29] A. Ansari, T. Murphey, Minimal parametric sensitivity trajectories for nonlinear systems, in: American Controls Conference (ACC), 2013.